AD-A146 785 SPICULES AND SURGES(U) STANFORD UNIV CA CENTER FOR SPACE SCIENCE AND ASTROPHYSICS M L BLAKE ET AL. 27 APR 84 N00014-75-C-0673 1/1

UNCLASSIFIED F/G 3/2 NL

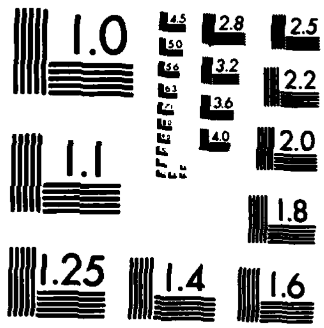

'OPY RESOLUTION TEST CHART

SPICULES AND SURGES

BY

M.L. BLAKE AND P.A. STURROCK[1]

Contract N00014-75-C-0673

CENTER FOR SPACE SCIENCE AND ASTROPHYSICS
STANFORD UNIVERSITY
Stanford, California

SPICULES AND SURGES

M.L. Blake and P.A. Sturrock[1]

Center for Space Science and Astrophysics

Stanford University, Stanford, California

Received: 1984 April 27; Accepted: ______________

Abstract

We adopt the position that spicules, macrospicules and surges are manifestations of the same phenomenon occurring on different scales. We therefore search for a mechanism that can be successfully applied to explain the phenomenon on all three scales.

We first consider the possibility that the mechanism is the same as that which operates in producing the solar wind, except that the divergence of the magnetic ducts is much more rapid. We find that the mechanism fails to explain spicules, macrospicules or surges. For instance, if it produces speeds typical of spicules, the maximum height is much too small; if it reproduces the height, the velocities are much too high. We also consider a variant of this mechanism proposed by Uchida in which the gas pressure is supplemented by the magnetic pressure of a gas composed of plasmoids. This mechanism also fails for similar reasons.

We have therefore re-examined the Pikel'ner mdoel, according to which gas is transported in a sequence of "magnetic sacks" which may for instance form as the result of reconnection, and we find that this model can reproduce the kinematic properties of spicules and surges. However, it is difficult to understand why the Pikel'ner mechanism, in its original form, could explain why spicules and surges are collimated. We propose that this is due to the involvement of two different magnetic-field configurations, one of which is

subject to reconnection and provides the driving force, the other of which provides the guidance necessary to explain the observed collimation.

We suggest that Ellerman bombs, which are associated with surges, are due to magnetic reconnection at or near the temperature-minimum region. We also suggest that coronal heating, outside of active regions, may be ascribed to dissipation of the currents which develop in the corona when the magnetic-field configurations associated with spicules erupt into the pre-existing magnetic field.

Subject headings: hydromagnetics - Sun: activity - Sun: activity - Sun: atmospheric motions - Sun: magnetic fields - Sun: solar wind

[1]Also Department of Applied Physics, Stanford University

I. Introduction

When the solar limb is observed with a narrow-band filter centered on one of the strong chromospheric emission lines (H or Ca II K), the chromosphere is observed to consist of many rapidly changing hairlike features called "spicules" (Beckers 1972). Each spicule appears to consist of a tube of diameter about 1,000 km extending to a height in the range 6,000-10,000 km, with a velocity in the range 20-30 km s^{-1}. The temperature is of order 10,000-20,000 K, and the density of order 3.10^{10} - $2.10^{11} cm^{-3}$. Each spicule appears to be ejected from the low chromosphere, and it may fall back along the same path or fade along its full length. The total lifetime is of order 5-10 m. Spicules occur continually on the surface of the sun; Beckers (1972) estimates that, at any time, there about 10^6 spicules on the sun's surface. It is now believed, on the basis of observations of spicules seen against the solar disk (Simon and Leighton 1964), that spicules tend to occur at the boundary of the supergranulation network. It is also worth noting that H bright mottles tend to occur at the roots of spicules (Beckers 1972).

In this article, we examine several possible mechanisms for spicules and also for surges (Svestka 1976; Tandberg-Hanssen 1974). When a flare starts, it is quite often accompanied by gas ejections which manifest themselves as moving prominences on the limb or Doppler-shifted dark filaments on the disk. One type of such ejection is a "surge", which typically has the form of a straight or slightly curved spike which grows upward from the chromosphere with velocities in the range 50-200 km s^{-1}. It reaches a maximum height in the range 20,000-200,000 km, and then fades or falls back to the chromosphere, apparently along the original trajectory. The lifetimes of these spikes are in the range 10-30 m. It appears that many surges are preceded by a diffuse expansion of a part of the flare. Roy (1973) has identified these expansions with "moustaches" or "Ellerman bombs".

Surges usually occur at small, changing satellite sunspots which represent islands of polarity reversal (Rust 1968) situated close to the edges of sunspot penumbrae (Giovanelli and McCabe 1958). When satellite sunspots disappear from the vicinity of a spot, surge activity ceases. It appears, therefore, that a surge is due to the magnetic field reversal of a satellite sunspot and that the process which gives rise to a surge also tends to eliminate the field reversal.

Apart from the differences in scales (length, time and velocity), there is a strong similarity between a spicule and a surge (Tandberg-Hanssen 1974). If a surge were scaled down in size and in velocity to values typical of spicules, it is probable that it would appear to be just another spicule.

In support of the proposition that spicules and surges are due to basically the same mechanism occurring on different scales, we also point out that there exist "macro-spicules". According to Beckers (1977), a macro-spicule resembles "a small surge" or a "giant spicule". These appear in the polar regions of the sun, rising to heights of up to 35,000 km with velocities of up to 150 km s^{-1}, lifetimes of up to 45 m, and diameters of up to 10,000 km. Hence the characteristic dimensions of macro-spicules bridge the gap between those of spicules and surges.

For the above reasons, we consider it reasonable to search for just one mechanism responsible for spicules, macro-spicules and surges. The appropriate values of physical parameters will vary from one category to another, but we assume that the same basic process occurs in all cases.

In searching for possible mechanisms of spicules and surges, we attach prime significance to the fact that the height of the spicule or surge is much greater than either the barometric scale height or the ballistic scale height for the relevant velocity. For temperatures usually quoted, the barometric scale height is in the range 300-600 km. The ballistic scale height $v^2/2g$ is only 1,300 km for a typical spicule velocity of 25 km s^{-1}, and is only 20,000 km for a typical surge velocity of 100 km s^{-1}. It is clear, therefore, that neither spicules nor surges can represent simple ballistic motion of chromospheric material ejected from the chromosphere. The material must be subject to an upward force which counteracts the effect of gravity.

It is also significant that this force must be comparable to the gravitational force. Gravity acting alone can reduce an initial flow velocity of 20 km s^{-1} to zero in a distance of only 700 km. Similarly, if the upward force were (for instance) twice that of gravity, an initial flow velocity of 20 km s^{-1} would be increased to 40 km s^{-1} in only 2,000 km, and is 70 km s^{-1} in 10,000 km. Hence the spicule mechanism must involve a force which is comparable with the force of gravity and remains fairly constant during the lifetime of a spicule. Similar remarks apply to surges.

In this article, we examine briefly three methods of providing the required auxiliary force. In Section II, we consider the possibility that a spicule is driven by the pressure of the spicule gas itself. In order to attain supersonic speeds, the spicule must then be produced by a mechanism analogous to that responsible for the solar wind (Parker 1963), which can be provided by an expanding magnetic flux tube. In order to simplify the analysis, we consider an idealized model in which the flow has achieved a steady state. We find that this model cannot produce flow heights much greater than one or two ballistic scale heights.

In Section III, we consider a proposal of Uchida (1969), which may be regarded as a modification of the above model. According to Uchida, the material flowing upwards in a spicule may be composed of many plasma bubbles or "plasmoids". In this case, the magnetic pressure of the plasmoid supplements the gas pressure. We follow Uchida in considering a steady-state flow; this involves only a slight extension of the analysis of Section II. Once again, we find that this model does not produce flow heights much greater than one or two ballistic scale heights.

The basic shortcoming of the above models is the following:- after acceleration to supersonic speeds at the "throat" of the expanding flux tube, the gas pressure and magnetic pressure become small so that the flow is almost ballistic. This directly contradicts one of the basic properties of spicules and surges, that the speed remains almost constant over lengths which are large compared with both the barometric scale height and the ballistic scale height. In consequence, if the models are to reproduce the observed heights, the maximum speeds are too high. If the maximum speeds are to be in agreement with observational data, the maximum heights are too small.

A variation of the hydrodynamic model has recently been proposed by Hollweg (1982). In this model, a train of shock waves travels along a magnetic flux tube, driving gas along the tube. The flow is ballistic between impulses, and quite high velocities (of order 60 km s^{-1}) are attained between impulses. Since spicules are so small, it is possible that their motion may be comprised of a sequence of impulsive steps, and that this would not be obvious from present-day observations. However, surges are much larger, so that the absence of observational evidence for the impulses required by the Hollweg model imply that the model is not applicable to surges. Since we are searching for a model which is applicable both to spicules and to surges, we are led to consider further models.

Pikel'ner (1969) presented a spicule model which differs in important respects from those we have discussed so far. The driving force is purely magnetic, and the magnetic field direction is transverse to the direction of motion. Although Pikel'ner proposed this mechanism only for spicules, we shall see that it is applicable also to surges. We have found, moreover, that the mechanism exhibits the great advantage that the accelerating force is, in a sense, self-stabilizing, leading to flows over substantial heights in which the acceleration is small in magnitude compared with the gravitational acceleration. If the magnetic field becomes too strong, the gas accelerates and the gas density therefore decreases: a decrease in gas density leads to a decrease in the magnetic field strength and therefore to a decrease in the acceleration. Conversely, if the magnetic field strength is too weak, the gas slows down; in consequence, the gas density and field strength increase so that the speed increases. A simple representation of this model, to be analyzed in Section IV, shows that the basic Pikel'ner mechanism can indeed lead to velocity profiles similar to those characteristic of spicules and surges.

II. Steady-State Hydrodynamic Flow

We consider steady flow along a thin flux tube which begins and returns to the chromosphere which thus provides both a source and a sink for the gas in the spicule. However, since the basic requirement of a spicule model is that it explain the upward motion of chromospheric gas, we shall restrict our attention to the initial upward motion and ignore the subsequent downward flow.

For simplicity, we consider steady upward flow along a thin vertical flux tube of which the area A is a given function A(z) of z, where z is measured in the upward direction. Then the equation of continuity is

$$nvA = J \quad , \tag{2.1}$$

where n is the particle number density, v the velocity, and J (the particle mass flux along the tube) is independent of z. All quantities are measured in c.g.s. units.

The equation of motion is

$$nmv \frac{dv}{dz} = - nmg - \frac{dp}{dz} \quad , \tag{2.2}$$

where m is the mean particle mass, g the (downward) gravitational acceleration and p the gas pressure, and the energy equation may be written as

$$\frac{3}{2} nkv \frac{dT}{dz} = - \frac{p}{A} \frac{d}{dz} (Av) + Q \quad , \tag{2.3}$$

where k is Boltzmann's constant, T is the temperature, and Q is the net rate of energy input per unit volume, taking account of energy loss by radiation. For the low temperatures and other conditions characteristic of spicules and surges, the role of thermal conduction in the energy equation may be ignored.

To the above equations we must add the relation

$$p = nkT \quad . \tag{2.4}$$

For the temperatures and other conditions of interest, ionization will play only a small role and will be neglected, so that the mass m to be the mass of a hydrogen atom, but we consider that there is sufficient ionization to insure that flow is along magnetic field lines.

We may use equation (2.4) to eliminate p, equation (2.1) to eliminate n, and then rearrange equations (2.2) and (2.3) to obtain expressions for dv/dz and dT/dz. The resulting equations are as follows:

$$\left(v - \frac{C^2}{v}\right)\frac{dv}{dz} = -g + \frac{C^2}{A}\frac{dA}{dz} - \frac{2}{3}\frac{AQ}{Jm} \tag{2.5}$$

$$\frac{3}{2}\left(1 - \frac{C^2}{v^2}\right)\frac{1}{T}\frac{dT}{dz} = \frac{g}{v^2} - \frac{1}{A}\frac{dA}{dz} + \left(\frac{5}{3} - \frac{C^2}{v^2}\right)\frac{AQ}{JmC^2} \quad , \tag{2.6}$$

where C is the sound speed defined by

$$C^2 = \frac{5kT}{3m} \quad . \tag{2.7}$$

We see that each of these equations has a "critical point" defined by the same conditions:

$$v_o = C_o \tag{2.8}$$

and

$$\frac{1}{A_o}\left(\frac{dA}{dz}\right)_o - \frac{g}{C_o^2} - \frac{2}{3}\frac{A_oQ_o}{JmC_o^2} = 0 \quad . \tag{2.9}$$

For given physical conditions, such as flux-tube geometry, heat input and radiation losses, one may view equations (2.8) and (2.9) as representing a regulating mechanism for the mass flux J.

For purposes of computing solutions of the above equations, it is convenient to introduce the following dimensionless variables,

$$\zeta = z/H_o \quad , a = A/A_o \quad , \xi = v/C_o \quad , \tau = T/T_o \quad , \mu = Q/Q_o \quad , \tag{2.10}$$

and the following dimensionless parameters,

$$\Gamma = gH_oC_o^{-2} \quad , \Lambda = \frac{2}{3}\frac{E_oA_oQ_o}{mJC_o^2} \quad . \tag{2.11}$$

In these expressions, E_o is the "expansion length" defined by

$$E_o^{-1} = \frac{1}{A_o}\left(\frac{dA}{dz}\right)_o \quad . \tag{2.12}$$

The quantity Γ is the ratio of the scale length characteristic of the expansion of the flux tube at the critical point to the ballistic scale height at the critical point. The quantity Λ may be viewed approximately as the ratio of the rate of energy input in the neighborhood of the critcal point to the kinetic energy flux at the critical point.

On introducing the Mach number

$$M = \frac{v}{c} \quad , \tag{2.13}$$

we may write equations (2.5) and (2.6) in the dimensionless form

$$(1 - M^{-2})\xi \frac{d\xi}{d\zeta} = - \Gamma + \frac{1}{a}\frac{da}{d\zeta} - \Lambda a \mu \tag{2.14}$$

and

$$\frac{3}{2}(1 - M^{-2}) \frac{d\tau}{d\zeta} = \Gamma \frac{\tau}{\xi^2} - \frac{1}{a}\frac{da}{d\zeta} + \frac{3}{2}\left(\frac{5}{3} - M^{-2}\right)\Lambda a \mu \, . \tag{2.15}$$

We see from equations (2.8) and (2.9) that the conditions at the critical point may now be expressed as

$$M_o = 1 \tag{2.16}$$

and

$$\Gamma + \Lambda = 1 \quad . \tag{2.17}$$

It follows from (2.17) that $\Lambda < 1$, i.e., that the expansion scale height H_o must be less than $C_o^2 g^{-1}$, which is twice the ballistic scale height corresponding to the speed of sound at the critical point. It also follows from (2.17) that $\Gamma < 1$, assuming that there is a net energy input at the throat so that $\Lambda > 0$.

We have computed solutions of equations (2.14) and (2.15) for a range of assumed forms for the area function A(z) and heating function Q(z). A typical solution is shown in Figure 1. For this particular case, the area A(z) is assumed to grow exponentially from the throat on, the expansion length being given by

$$\left.\begin{array}{lll} E = \infty , & & \text{for } z < 0 , \\ E = 500 \text{ km} , & & \text{for } 0 \leq z < 2000 \text{ km} , \\ E = 5000 \text{ km} , & & \text{for } z \geq 2000 \text{ km} . \end{array}\right\} \quad (2.18)$$

For the heating function, we adopt the gaussian form

$$Q(z) = Q_o \exp\left(\frac{-(z - z_p)^2}{H_w{}^2}\right) , \qquad (2.19)$$

which peaks at the value z_p and has a width determined by H_w.

The velocity v(z) and temperature T(z) resulting from this model are shown in Figure 1. It is to be noted that the temperature decreases very rapidly, due to adiabatic expansion. The velocity increases for temperatures greater than 10,000 K but decreases rapidly when the temperature drops below 10,000 K. It is clear that this particular model does not meet the requirement of a spicule model, that the velocity remains constant over several ballistic scale heights.

The above result is not peculiar to the case specified by equations (2.18) and (2.19); it seems to be quite general. This property of the hydrodynamic model may be understood as follows. In order for the flow to continue to accelerate after it becomes supersonic, the equation of motion (2.14) must be dominated either by the expansion term $(1/a)\,(da/d\zeta)$ becoming large and positive, or by the heating term $\Lambda a\mu$ becoming large and negative (representing a large heat loss by radiation). In either case, we see from equation (2.15) that the effect is to lead to a negative value of $d\tau/d\zeta$, so that the temperature decreases with height. However, if the temperature decreases with height, the expansion term in equation (2.14) will soon become negligible. The flow then becomes essentially ballistic. Ballistic flow and a decrease in temperature with height are both inconsistent with spicule observations (Beckers 1972).

This model also fails to reproduce the properties of surges. In order to attain heights characteristic of the largest surges ($\sim 10^{10}$ cm), we require that $C_o^2/2g$ attain this value. This then requires that $C_o \simeq 10^{7.4}$, which in turn requires a temperature $T \simeq 10^{6.3}$. This temperature is much higher than the temperature of surge material, which is of order 10^4 K.

III. Modified Uchida Model

Uchida (1969) has considered a model which is a variant of that considered in Section II. He considers that plasmoids are produced during the reconnection process, each plasmoid containing gas and a closed magnetic field. The gas pressure is then supplemented by magnetic pressure.

In this section, we follow Uchida in this general concept. However, Uchida assumes that the magnetic field strength of the plasmoids is a known function of height. We prefer to estimate the magnetic field strength of the plasmoids by an "equation of state". We assume that the magnetic field is "frozen" into the plasma. Then the manner in which the magnetic field changes, in response to a change in the gas, depends on what assumptions one makes concerning the relative directions of expansion and of the magnetic field. For instance, if the expansion is along the magnetic field, then B is independent of the gas density n. If, on the other hand, the expansion is transverse to the magnetic field, then B is proportional to n.

We assume that the magnetic field is statistically isotropic, from which it follows that $B \propto n^{2/3}$. Since the magnetic pressure is proportional to B^2, it follows that

$$p_m \propto n^{4/3} \quad , \tag{3.1}$$

so that

$$\frac{p_m}{p_{m,o}} = \left(\frac{n}{n_o}\right)^{4/3} \quad , \tag{3.2}$$

where $p_{m,o}$ and n_o will be interpreted as the values at the "throat". On using equations (2.1) and (2.10), (3.2) becomes

$$p_m = p_{m,o}\, a^{-4/3}\, \xi^{-4/3} \quad . \tag{3.3}$$

The analysis of this section follows closely that of the previous section. The equation of continuity (2.1) and the energy equation (2.3) are unchanged. However, the equation of motion (2.2) is now replaced by

$$nmv \frac{dv}{dz} = - nmg - \frac{dp}{dz} - \frac{dp_m}{dz} \quad . \tag{3.4}$$

Another effect of the magnetic pressure is to change the wave-propagation speed, so the speed of sound C is now replaced by K, where

$$K^2 = C^2 + \frac{2}{3} V_A{}^2 \quad , \tag{3.5}$$

where C is the speed of sound defined in equation (2.7), and V_A is the Alfven speed defined by

$$V_A{}^2 = \frac{B^2}{4\pi nm} \quad . \tag{3.6}$$

The "Mach number" will now be defined as

$$M = \frac{v}{K} \quad . \tag{3.7}$$

In equations (2.10) and (2.11), C_o is now replaced by K_o, so that the dimensionless variables and parameters become

$$\zeta = z/H_o \quad , a = A/A_o \quad , \xi = v/K_o \quad , \tau = T/T_o \quad , \mu = Q/Q_o \quad , \tag{3.8}$$

and

$$\Gamma = gE_oK_o^{-2} \quad , \Lambda = \frac{2}{3}\frac{E_oA_oQ_o}{mJK_o^2} \quad . \tag{3.9}$$

We also introduce the symbol

$$\theta = (K/K_o)^2 \quad , \tag{3.10}$$

which may be viewed as a normalized "effective temperature".

With this terminology, we now obtain, in place of (2.14) and (2.15), the equations

$$(1 - M^{-2})\xi \frac{d\xi}{d\zeta} = -\Gamma + \theta \frac{1}{a}\frac{da}{d\zeta} - \Lambda a \mu \qquad (3.11)$$

and

$$\frac{3}{2}(1 - M^{-2})\frac{d\tau}{d\zeta} = \Gamma \frac{\tau}{\xi^2} - \tau \frac{1}{a}\frac{da}{d\zeta} + \frac{5}{2}\Lambda\left(1 - M^{-2} + \frac{2}{5}\frac{\tau}{\xi^2}\right) \quad . \qquad (3.12)$$

We see that this pair of equations also allows a transition from subsonic to supersonic flow at a critical point at which equations (2.16) and (2.17) must be satisfied.

Numerical solutions of these equations are shown in Figure 2, representing a case with moderate magnetic field strength. The magnetic stress leads to higher peak velocities and greater heights of the flow patterns. As before, rapid cooling occurs in the expansion region, and the motion is essentially ballistic beyond the height at which the velocity has its maximum value. The maximum velocity (50 km s^{-1}) is larger than is typical of spicules, yet the model does not extend to heights typical of spicules. We have also considered a similar case with strong magnetic field. This produced a flow pattern extending almost to 15,000 km, but the maximum velocity was found to be 75 km s^{-1}, much higher than is typical of spicules. From these and other examples, it is clear that the Uchida model does not meet the requirements of a valid model of spicules.

We have also investigated the possibility that the Uchida model may represent the mechanism of surges. However, the model fails for the same reasons that it fails to explain spicules. If the speed is correct, the height is too small; if the height is correct, the speed is too high.

IV. Simulation of the Pikel'ner Mechanism

We wish to consider the dynamics of a plasma-magnetic-field configuration proposed by Pikel'ner (1969), which could result from the reconnection at the chromospheric level of a vertical current sheet. We adopt the simplest model of this system shown in Figure 3. We suppose, for simplicity, that the density of gas in the corona is sufficiently small that it may be neglected. We also assume that the temperature of the gas trapped in the magnetic field is sufficiently low that the gas pressure may be neglected. The gas then forms a thin sheet in the vertical plane. The actual thickness of the sheet will be discussed briefly in Section V.

We assume that the plasma-field configuration is uniform in the y-direction and symmetrical about the plane $x = 0$, the z-axis being in the vertical direction. We also assume that $B_y \equiv 0$. Since we are assuming that the density of plasma may be neglected away from the boundaries $z = 0$ and $x = 0$, the magnetic field will be current-free away from these boundaries.

It is convenient to describe the magnetic field by ψ, the y-component of the vector potential:

$$B_x = -\frac{\partial \psi}{\partial z} \quad , \quad B_z = \frac{\partial \psi}{\partial x} \quad . \tag{4.1}$$

Then

$$\frac{\partial^2}{\partial x^2} + \frac{\partial^2 \psi}{\partial z^2} = 0 \tag{4.2}$$

away from the boundaries $z = 0$ and $x = 0$. In addition, ψ is constant along any field line, and therefore labels the field lines. We assume that the horizontal surface $z = 0$ is perfectly conducting. Hence ψ will be fixed in the plane $z = 0$.

We assume that the cool gas of the spicule is highly conducting and initially distributed in the plane $x = 0$. If the magnetic field is symmetrical, then the gas will always be in the plane $x = 0$. Furthermore, the magnetic field lines will move with the gas, so that ψ may be used to label elements of the gas. Motion of the gas may therefore be described by the function

$$z = Z(\psi, t) \quad . \tag{4.3}$$

If $R(\psi)\, d\psi\, dy$ is the mass of gas with ψ in the range ψ to $\psi +\ d\psi$ and y in the range y to $y + dy$, the surface mass density σ is given by

$$R(\psi)\, d\psi = \sigma(z,t)\, dz \quad , \tag{4.4}$$

the arguments of the variables being related by (4.3).

The equation of motion of the gas is given by

$$\frac{d^2Z}{dt^2} = - g - \sigma^{-1} J_y B_x \quad , \tag{4.5}$$

where g is the downward gravitational acceleration and J_y is the surface current density in the plane $x = 0$. This equation may be expressed in terms of the vector potential ψ:

$$\frac{d^2Z}{dt^2} = - g - \frac{1}{2\pi\sigma} \left(\frac{\partial\psi}{\partial z}\right)_0 \left(\frac{\partial\psi}{\partial x}\right)_{0+} \quad , \tag{4.6}$$

in which $(\partial\psi/\partial z)_0$ is evaluated at $x = 0$ and $(\partial\psi/\partial x)_{0+}$ is evaluated at $x = > 0$.

For the purpose of computing the evolution of this system, it is convenient to work with a finite volume. As shown in Figure 3, we introduce additional fictitious conducting boundaries at $x = \pm L$ and $z = L$, where L is chosen to be large compared with the dimensions of the spicule model.

The results of the simulation for typical spicule parameters are shown in Figure 4, where Figure 4a shows the trajectories of individual spicule particles. The simulation begins after the assumed reconnection has occurred, with the spicule material traveling at a velocity of 25 km s^{-1} and with the spicule material resting on reconnected magnetic field lines. Acceleration due to the magnetic stress increases the spicule velocity to 36 km s^{-1}, with a corresponding ballistic scale height of 2400 km. The flow length is 8000 km for the upper part of the spicule, significantly greater than the ballistic scale height.

Figure 4b shows the magnetic field at the beginning of the simulation and Figure 4c shows the field after 250 seconds. A line dipole is used to produce the initial field. As the field lines are symmetric about $x = 0$, we show only the field lines in the region $x > 0$. Because of the symmetry, there is a reversal in the z component of the magnetic field at the $x = 0$ boundary and, consequently, a current sheet at this boundary. At 250 seconds (Figure 4c), the spicule material has reached its maximum height and has begun falling back to the chromosphere.

This simulation can also model surges. If the size of the magnetic loop, the magnetic field strength, the initial velocity and the surface density are increased, the resultant motion is characteristic of a surge. Figure 5a shows the trajectories of various particles. The velocity (50 km s^{-1}) and height (120,000 km) are characteristic of small surges. Figure 5b shows the magnetic field at $t = 0$, and Figure 5c shows the magnetic field lines at 1000 seconds, when the surge is near its maximum height.

V. Discussion

We have shown that two of the conceptually simplest models of spicules and surges (Section II and III) fail to reproduce their properties. Both phenomena require that the gas move under the influence of a force which almost balances the force of gravity over a height which is much larger than the barometric scale height and much larger than the ballistic scale height. Neither of the models provides such a force. Even if the above models had been able to reproduce the velocity curves of spicules and surges, they would have encountered another difficulty. In order to accelerate gas in a duct to supersonic speeds, it is necessary that the duct expand. The transverse dimension of the gas would therefore expand with height. However, observational data indicate that the transverse dimension of spicules, if anything, decreases with height (Beckers 1972).

By contrast, we have seen in Section IV that the Pikel'ner model is capable of yielding trajectories consistent with those found for both spicules and surges. (Intermediate ranges of the parameters should reproduce the trajectories of macrospicules.) This model involved many approximations, one of which was the assumption that gas in the spicule has zero temperature. According to this assumption, a spicule or surge has the structure of an infinitely thin sheet. If the assumption of zero temperature is relaxed, the sheet will acquire a finite width. The thickness of this sheet may be estimated simply if one assumes that the thickness is small compared with the scale of variation of the structure in the vertical direction, and that the time scale of the variation of the cross-sectional structure is long compared with the dynamical relaxation time. Then a relevant model is that of a static plasma-magnetic-field configuration, uniform in the z-direction, in which the plasma is supported at the bottom of open magnetic field lines which are concave in the upward direction (Kippenhahn and Schlüter 1957). It has been shown that, if the gas is assumed to be isothermal, the above conditions are met by the following model:

$$B_x = B_o \cos \phi \tag{5.1}$$

$$B_z = B_o \sin \phi \tanh (x/W) \tag{5.2}$$

$$p = p_o \operatorname{sech}^2 (x/W) \tag{5.3}$$

$$\rho = \rho_o \operatorname{sech}^2 (x/W) \tag{5.4}$$

in which p_o and ρ_o are related by

$$p_o = \frac{kT}{m} \rho_o \quad , \tag{5.5}$$

where T is the temperature and m is the mean particle mass. In this model, magnetic field lines tend asymptotically to straight lines inclined at an angle ϕ to the horizontal axis.

The quantity W, which is a measure of the width of the sheet, is given by

$$W = 2H \cot\phi \quad , \tag{5.6}$$

where H is the normal barometric scale height defined by

$$H = \frac{kT}{mg} \quad . \tag{5.7}$$

In estimating the thickness of the sheet, one may of course include the effect of acceleration in the gravitational term g.

As an example, we may consider that the gas temperature is 10^4 K, and that the effect of acceleration is small so that g may be taken to be

$10^{4.4}$ cm s^{-2}. Noting that, at that temperature, the mean particle mass is approximately the mass of a hydrogen atom, we see that $H = 10^{7.5}$ cm. If $\phi = \pi/4$, then $W = 10^{7.8}$ cm so that the total width $2W$ is of order 1,000 km. This estimate is sufficiently small that our model is consistent with the observed widths of spicules. The observed widths of surges are much larger than 1,000 km; however, a wide sheet of thickness only 1,000 km would appear, in a typical projection, to be much larger than 1,000 km.

We have stressed in earlier sections that the heights attained by spicules and surges exceed the relevant ballistic scale heights. Furthermore, the velocity tends to be fairly steady. This implies that the net force acting on the spicule or surge material is substantially less than the gravitational force. Hence, one must look for a regulating mechanism which leads to a subsequent near-balancing of the magnetic and gravitational forces. It appears that the Pikel'ner model provides such a regulating mechanism. If the magnetic force is larger than the gravitational force, the material will accelerate in the upward direction. Since the magnetic field lines are "frozen" into the material, the field strength will decrease as the velocity increases, so that the magnetic force will diminish. Conversely, if the magnetic force drops below the gravitational force as the material travels outwards, the velocity will decrease, leading to an increase in both the field strength and the magnetic force.

Although the present model involves a sheet of gas which moves coherently and appears for this and other reasons to be consistent with the observed properties of spicules and surges, this coherence may possibly be a consequence of the assumed symmetry of the configuration. In a more realistic situation, which is not highly symmetrical, the flow may not be coherent. It is possible that different groups of magnetic field lines would move in different directions so that an initially coherent mass of gas would disperse and perhaps even fragment. Such behavior is characteristic of flare sprays, and it seems to us likely that the Pikel'ner model, if it were applied to more realistic initial conditions and boundary conditions, would lead to a fragmented eruption, and would therefore provide a realistic model of a spray.

In view of the above concerns, we consider it possible that something else is required to explain the apparent channeling of the material which erupts in the course of a spicule or surge. Concerning surges, for which there is better observational data, we have noted the following conflict:- the trajectory (height as a function of time) agrees quite well with the Pikel'ner model in which the magnetic field is transverse to the trajectory. On the other hand, cinematograph data gives the appearance of gas moving parallel to magnetic field lines.

In an attempt to resolve this paradox, we have obtained copies of photographs of a surge taken at times of unusually good seeing, by courtesy of Sacramento Peak Observatory. One of these photographs is reproduced as Plate I. Examination of these prints has led us to the conclusion that this particular surge involved the interplay of two distinct magnetic-field configurations. One set of field lines runs parallel to the trajectory of the surge. The other set of field lines is transverse to the former. The model which this suggests is that a surge is represented by the evolution of a magnetic-field pattern similar to that described in Section IV, but these field lines were constrained by, and therefore guided by, another set of field lines, as indicated schematically in Figure 6. This configuration appears to be quite compatible with the fine structure of the surge shown in Plate I. It is not an unreasonable situation to occur low in the sun's atmosphere at heights characteristic of spicules, or even at greater heights in the vicinity of active regions which provide the environment in which surges occur. It is likely that, in both these situations, most of the magnetic flux is comprised of closed magnetic field lines. If part of this magnetic field is somehow disconnected from the photosphere, it may tend to move as described in the Pikel'ner model. However, it will be moving in an environment of a closed magnetic field tied to the photosphere. We conjecture that the interplay of the moving, released field with the "anchored" field will provide a situation of the type shown in Figure 6.

The Pikel'ner model, in its original form, could be simplified sufficiently that it could be studied in a 2-D model. However, if a surge or spicule involves the interplay of two magnetic-field configurations, as indicated schematically in Figure 6, we are faced with an intrinsically 3-D problem which will be very difficult to pursue either analytically or numerically.

We are now left with the problem of trying to understand why, in certain configurations, the magnetic-field eruption is guided and leads to a surge (or, on a smaller scale, to a spicule) whereas, in other cases, the eruption is not constrained by the surrounding magnetic field and leads to a spray. This question needs further study, but there appear to be at least two possible answers:- one possibility is that surges occur in a center of activity where the magnetic field lines are predominantly closed, whereas sprays occur in centers of activity where the magnetic field lines are predominantly open. Another possibility is that the higher velocities characteristic of sprays lead to sufficiently high kinetic energies of the ejected gas that the motion is not constrained by the surrounding magnetic field; for the lower velocities characteristic of surges, this situation may not arise.

It is also possible that the difference between surges and sprays rests in the original magnetic-field release process. Sprays are typically produced by flares. The initiation of a surge appears to be related either to a flare or to an Ellerman bomb. (In this context, it is worth noting that there is some evidence, from H alpha observations on the disk and from CaII K observations on the limb, that there are brightenings at the base of spicules [Beckers 1972].) An Ellerman bomb (Martres and Bruzek 1977) differs from a flare in that the radiation comes from deeper in the sun's atmosphere (resulting in a "moustache"-like spectrum) and the radiation is slower and steadier. Hence, further study of the spicule-surge problem necessarily involves an attempt at understanding the Ellerman-bomb process. At this time, we see two possibilities:- one is that the magnetic-field release process characteristic of surges and spicules is magnetic-field reconnection (as proposed by Pikel'ner), but that the reconnection occurs much deeper in the sun's atmosphere than is normal for flares. Alternatively, Ellerman bombs may be the manifestation of anomalously rapid slippage of magnetic field lines through the upper photosphere and chromosphere, perhaps by the resistive Rayleigh-Taylor instability discussed by Coppi (1964). The latter interpretation explains the close association between the disappearance of satellite sunspots and the termination of surge activity.

It should be possible to arrive at a definitive answer to our proposal that spicules and surges involve basically the same mechanism, by observations which could be made with the Solar Optical Telescope. It should be possible to determine (a) whether there is a small region of reverse magnetic polarity at the base of each spicule; (b) whether brightenings, similar to Ellerman bombs, occur at the base of each spicule; and (c) whether the range of morphologies of spicules is similar to that of surges.

In the case of a surge, the size of the "satellite sunspot" producing the polarity-reversal region is of order 10^8 - $10^{8.5}$ cm (1 - 3 arc sec). It requires $10^{1.5}$ gauss to support gas of density 10^{11}cm^{-3} extending over a height 10^{10} cm. If the cross-sectional dimension of the surge is 10^9 cm, the required magnetic flux is of order $10^{19.5}$ Mx. This is the flux in an area of diameter 10^8 cm if the field strength is $10^{3.5}$ gauss, or in an area of diameter $10^{8.5}$ cm if the field strength is $10^{2.5}$ gauss. For a typical spicule, the height is less by a factor of about 10, so that the required field strength is of order 10 gauss. Furthermore, the cross-sectional dimension is of order 10^8 cm, so that the required flux is only 10^{17} Mx. This amount of flux would be contained in a spot of diameter $10^{7.5}$ cm if the field strength is $10^{2.5}$ gauss, or in a spot of diameter 10^7 cm if the field strength is 10^3 gauss. It has become clear in recent years, from observations made by Sheeley (1967) and others (see, for a summary, Parker [1979]) that a large fraction of the magnetic flux penetrating the photosphere is contained in small regions (size of order $10^{7.4}$cm) of high field strength (of order $10^{3.2}$ gauss). Hence it is quite possible that the small regions of reverse polarity required to produce spicules, according to the present picture, would escape detection by conventional telescopic methods. However, it should be possible to detect such regions by means of the Solar Optical Telescope.

Despite the high resolution to be expected of SOT, it is very unlikely that one will obtain sufficiently fine detail to be able to check the assumption that spicules, as well as surges, involve the interplay of two different sets of magnetic-field lines. However, photographs of surges made by means of SOT should give much clearer indication of the magnetic structure associated with a surge, and hence should confirm or disprove our conjecture that surges (and - by analogy - spicules) involve the interplay of two systems of magnetic field lines.

By accepting observational evidence that the magnetic field at the photospheric level is confined in small knots of strong magnetic field, we may make a simple estimate concerning our proposed interpretation of Ellerman bombs (Martres and Bruzek 1977). If reconnection occurs near the photosphere, the logical location is the height at which the electrical conductivity is a minimum. This occurs approximately at the temperature minimum region where (Allen 1973) $T \approx 4200$ and $n_H \approx 10^{15.2}$. In consequence, one finds that the electrical conductivity σ (modified gaussian units) has the value $\sigma = 10^{0.7}$. Hence the magnetic diffusion coefficient D ($cm^2 s^{-1}$), given by

$$D = \frac{c}{4\pi\sigma} \quad , \tag{5.8}$$

has the value $D = 10^{8.7}$. By adopting the value $10^{7.4}$ for the radius r (cm) of a magnetic knot, we find that the characteristic diffusion time τ_D (s), given by

$$\tau_D = D^{-1} r^2 \quad , \tag{5.9}$$

has the value $10^{6.1}$. By adopting $B = 10^{3.2}$, we find that the Alfvén speed V_A (cm s^{-1}) has the value $10^{7.0}$, so that the Alfvén travel time τ_A (s), the time it takes an Alfvén wave to travel the characteristic distance r, is $\tau_A = 10^{0.4}$. According to the linear tearing-mode theory of Furth, Killeen and Rosenbluth (1963), the reconnection time is given approximately by

$$\tau_R \approx \tau_A^{1/2} \tau_D^{1/2} \quad . \tag{5.10}$$

On adopting the above values of τ_A and τ_D, we estimate that the reconnection time is about $10^{3.3}$ s, i.e., about 30 m. The lifetimes of Ellerman bombs are found to range from several minutes to a few hours, which is compatible with our estimate if some bombs involve even smaller magnetic knots, and some involve several knots, as would be required to produce a detectable "satellite sunspot".

Finally, we wish to point out that our proposed interpretation of spicules suggests a new mechanism for coronal heating. It is known that the kinetic energy carried into the corona by spicules is too small to account for the required energy input into the corona (Athay 1976). However, we are regarding the visible spicule as resulting from the eruption of a small amount of magnetic flux that has become detached from the photosphere by reconnection. The eruption of magnetic flux into the corona, which is already permeated by magnetic field, will lead to current sheets at the interface between the old field and the new field. If the magnetic field in the corona contains currents, it necessarily contains free energy which may be released by reconnection. We conjecture that this may be the process which heats the corona outside active regions.

According to our model, the dimension of the magnetic field configuration responsible for a spicule is much larger than the dimension of the visible spicule. Hence the free energy which results from the magnetic-field eruption may be substantially larger than the energy required to produce a spicule. We are therefore making a fairly conservative estimate of the rate at which energy is injected into the corona by considering the energy required to produce a typical visible spicule, and multiplying this by the rate at which spicules occur over the sun. From the parameters quoted in the introduction, we see that a typical spicule mass is $10^{12.2}$ g and a typical height is 10^9 cm.

Hence each spicule requires about $10^{25.6}$ erg to account for the gravitational energy. By noting that the average spicule lifetime is about $10^{2.7}$ s, and that there are normally about 10^6 spicules over the face of the sun, we find that the rate at which energy is being injected into the corona may be conservatively estimated to be $10^{28.9}$ erg s^{-1}, corresponding to an average energy flux of $10^{6.2}$ erg cm $^{-2}s^{-1}$. From this simple estimate, it appears possible that, outside active regions, the corona is heated by the dissipation of currents which are produced by the eruption of magnetic flux associated with spicules.

This work was supported in part by NASA Grants NGL 05-020-272 and NAGW-92 and the Office of Naval Research Contract N00014-75-C-0673.

References

Allen, C.W. 1973, Astrophysical Quantities (London, Athlone Press), p. 165.

Athay, R.G. 1976, The Solar Chromosphere and Corona: Quiet Sun (Holland, Reidel), p. 384.

Beckers, J. M. 1972, Ann. Rev. Astron. Astrophys., 10, 73.

Beckers, J. M. 1977, Illustrated Glossary for Solar and Solar-Terrestrial Physics (eds. A. Bruzek and C.J. Durrant; Dordrecht, Holland: Reidel), p. 32.

Coppi, B. 1964, Ann. Phys., 30, 178.

Furth, H.P., Killeen, J., and Rosenbluth, M.N. 1963, Phys. Fluids, 6, 459.

Giovanelli, R. G., and McCabe, M. 1958, Australian J. Phys., 11, 191.

Hollweg, J. V. 1982, Ap. J., 257, 345.

Kippenhahn, R., and Schlüter, A. 1957, Zs. Ap., 43, 36.

Martres, M.J., and Bruzek, A. 1977, Illustrated Glossary for Solar and Solar-Terrestrial Physics (eds. A. Bruzek and C.J. Durrant; Dordrecht, Holland, Reidel), p. 53.

Parker, E. N. 1963, Interplanetary Dynamical Processes (New York: Interscience).

Parker, E. N. 1979, Cosmical Magnetic Fields (Oxford: Clarendon Press), pp. 207 et seq.

Pikel'ner, S. B. 1969, Sov. Astron. AJ, 13, 259.

Roy, J. R. 1973, Solar Phys., 28, 95.

Rust, D. M. 1968, Structure and Development of Solar Active Regions, (ed. K. O. Kiepenheuer; Dordrecht, Holland: Reidel), p. 77.

Sheeley, N. R. 1967, Solar Phys., 1, 171.

Simon, G. W., and Leighton, R. B. 1964, Ap. J., 140, 1120.

Svestka, Z. 1976, Solar Flares (Dordrecht, Holland: Reidel), p. 221.

Tandberg-Hanssen, E. 1974, Solar Prominences (Dordrecht, Holland: Reidel), p. 103.

Tandberg-Hanssen, E. 1977, Illustrated Glossary for Solar and Solar Terrestrial Physics (eds. A. Bruzek and C. J. Durrant; Dordrecht, Holland: Reidel), p. 106.

Uchida, Y. 1969, Pub. Astron. Soc. Japan, 21, 128.

Figure Captions

Figure 1 Hydrodynamic model with the critical temperature equal to 20,000 degrees. The expansion and heating functions are shown in figure 1a. The velocity, shown as a function of height in figure 1b, decays in a distance comparable to the ballistic scale height of the maximum velocity. The temperature also is shown in figure 1b; note the rapid cooling that occurs due to the large expansion near the throat.

Figure 2 Uchida model with moderate magnetic field (V_A=10 km s^{-1}, C_0=25 km s^{-1} at the critical point). Comparing this with figure 1, we find a larger peak velocity and spicule height due to the magnetic force. As in the hydrodynamic model, rapid cooling occurs in the expansion region, and the motion is essentially ballistic past the peak velocity.

Figure 3 The Lorentz (magnetic) force driving the vertical motion of spicule material (shown along the axis of symmetry) is derived from a two-dimensional model of the magnetic field. The broken lines represent magnetic field lines that have recently reconnected at chromospheric height and support the spicule material derived from the chromosphere. Both sets of solid lines represent magnetic field lines that were unaffected (topologically) by the reconnection process. The photosphere at $z = 0$ is assumed to be perfectly conducting, and additional fictitious fixed conducting surfaces are introduced at $z = L$ and $x = \pm L$.

Figure 4 Simulation of a spicule. (a) Trajectories of particles which begin with velocities of order 25 km s^{-1}, attributed to the original reconnection process. It is seen that the material attains a height of almost 13000 km and that the maximum velocity is only about 35 km s^{-1}. These values are comparable with those characteristic of spicules. (b) The initial magnetic field at t = 0. The field has strength of about 6 gauss at the lower boundary. (c) The magnetic field at t = 250 s.

Figure 5 Simulation of a surge. (a) Trajectories of particles for typical surge parameters. The initial velocity is about 50 km s^{-1}, attributed to the reconnection process. The material attains a height of almost 15,000 km, and the maximum velocity is about 120 km s^{-1}. (b) The initial magnetic field at t = 0. The magnetic field strength at the lower boundary is about 20 gauss. (c) The magnetic field at t = 1,000 s.

Figure 6 Proposed magnetic-field configuration for surges, based on the $H\alpha$ photograph of a surge shown in Plate I. The configuration involves two distinct sets of magnetic field lines: group A represents a "passive" configuration of field lines firmly anchored in the photosphere; group B represents an "active" configuration of field lines which have become detached from the photosphere by reconnection. Group B supports cool gas and also provides the force required to move the gas. Group A provides the "magnetic rail" constraining the motion of the magnitic field lines of group B. Since the cool gas is trapped at the bottom of the field lines of group B, the combined effect is that of gas traveling along the magnetic field lines of group A.

Plate I. Surge appearing on the limb of the sun on 1982 November 24, photographed in Hα light, provided by courtesy of Sacramento Peak Observatory.

MICHAEL L. BLAKE: Abrams, Apt. 2E, Escondido Village, Stanford University, Stanford, CA 94305

PETER A. STURRROCK: Center for Space Science and Astrophysics, ERL 306, Stanford University, Stanford, CA 94305

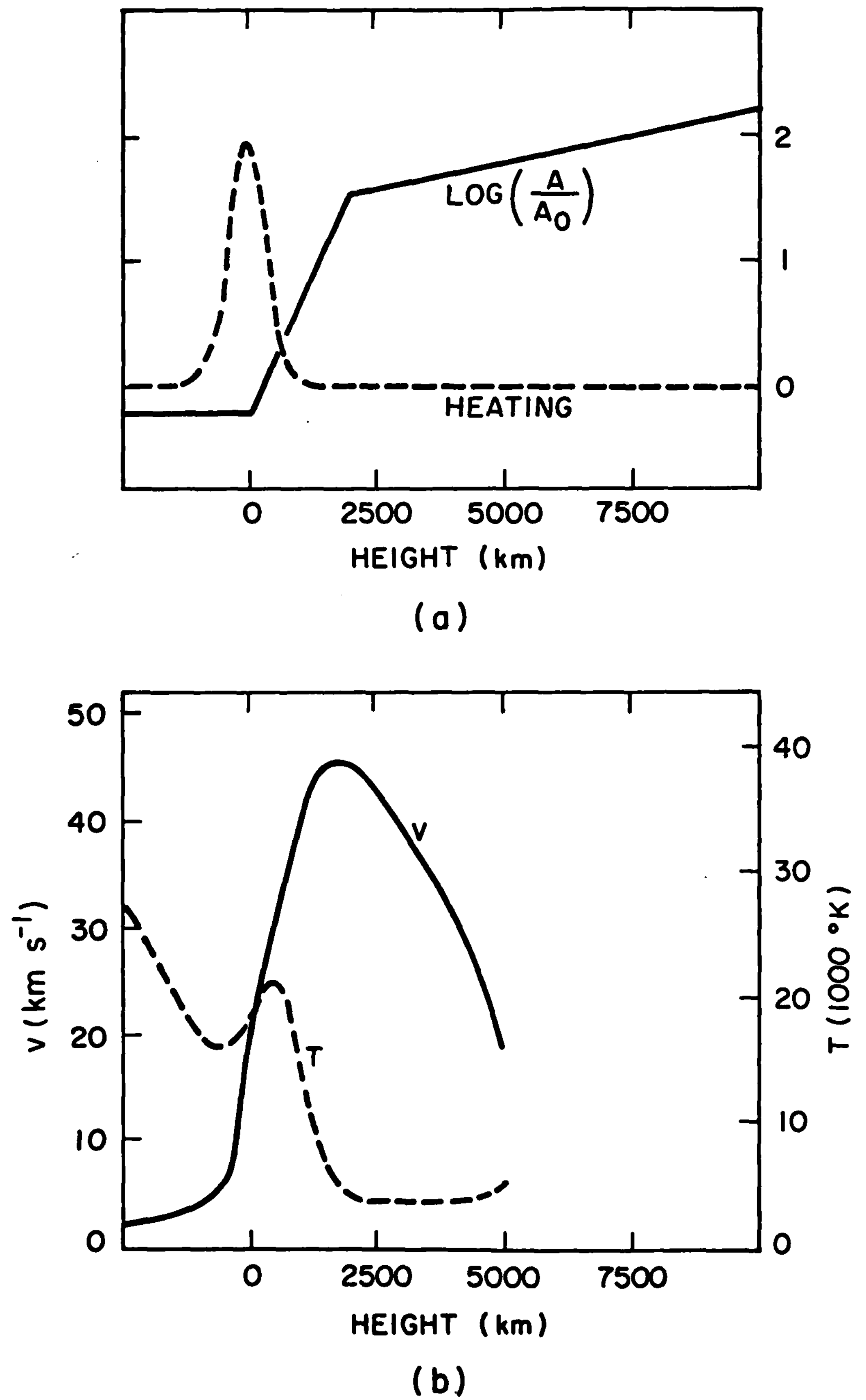
LOG $\left(\frac{A}{A_0}\right)$
HEATING
2
1
0
0
2500
5000
7500
HEIGHT (km)
(a)
50
40
30
20
10
0
v (km s^{-1})
V
T
40
30
20
10
0
T (1000 °K)
0
2500
5000
7500
HEIGHT (km)
(b)

Figure 1

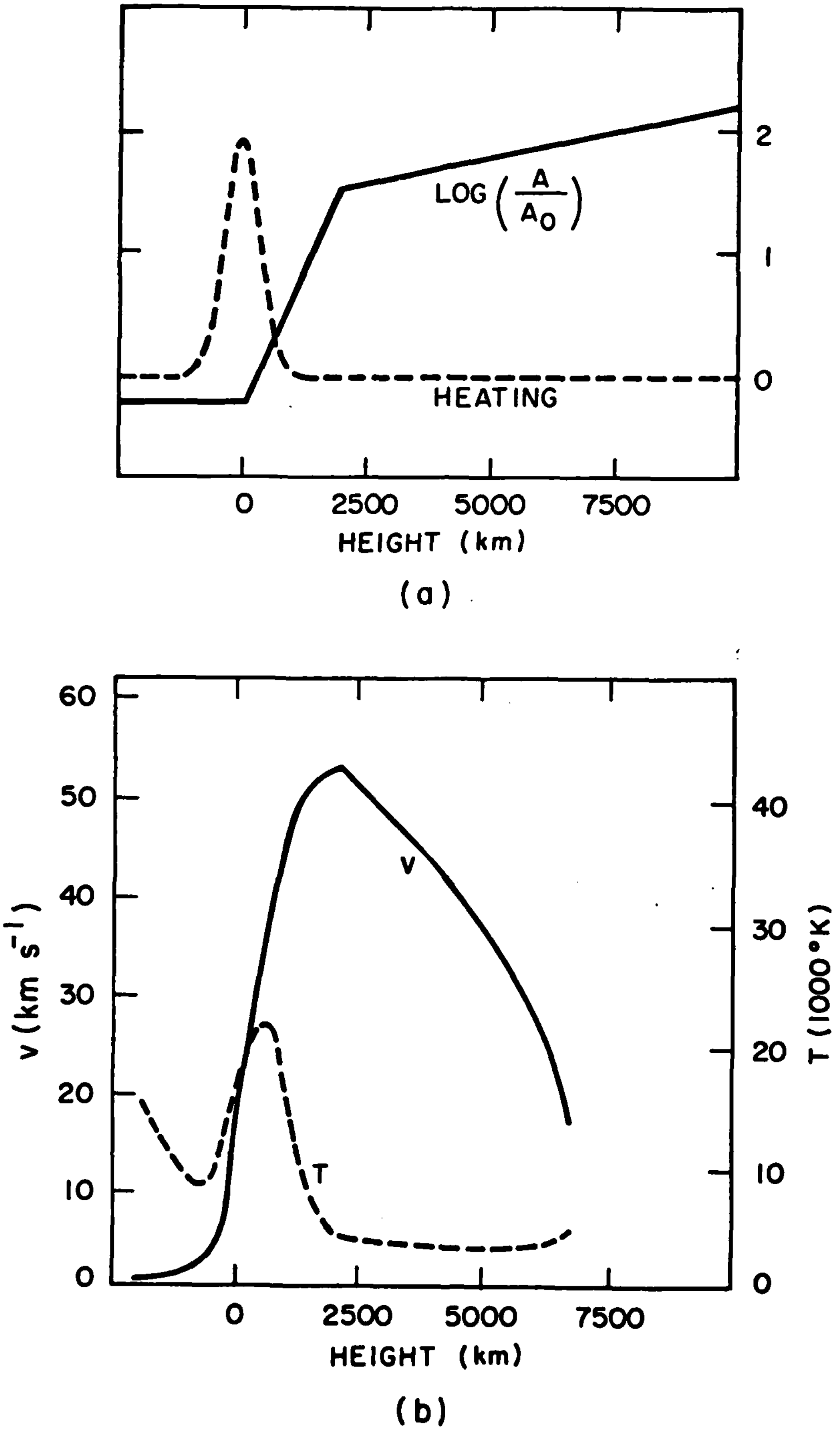
LOG $\left(\frac{A}{A_0}\right)$
HEATING
2
1
0
0
2500
5000
7500
HEIGHT (km)
(a)
60
50
40
30
20
10
0
v (km s^{-1})
V
T
40
30
20
10
0
T (1000 °K)
0
2500
5000
7500
HEIGHT (km)
(b)

Figure 2

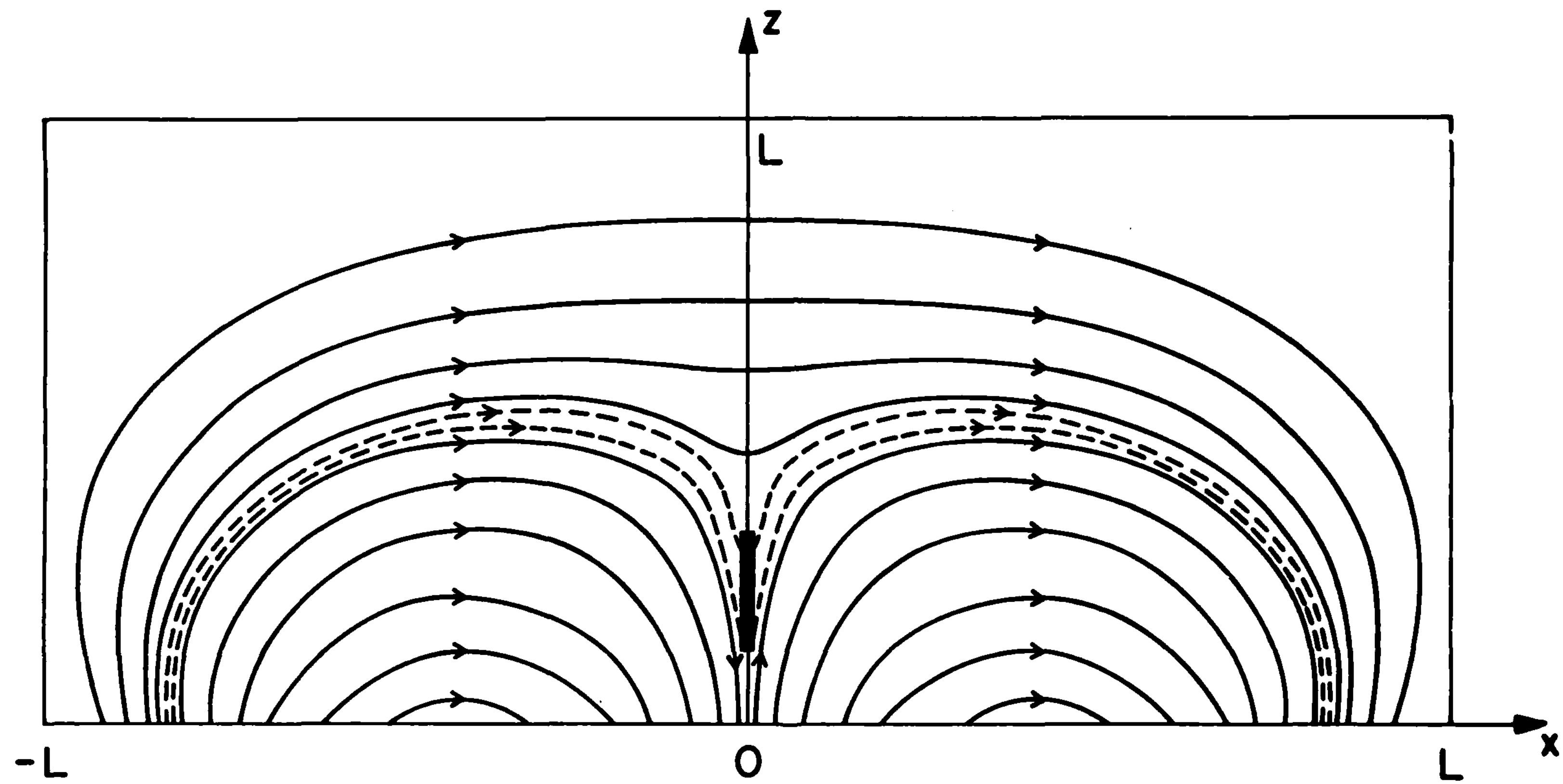

Figure 3

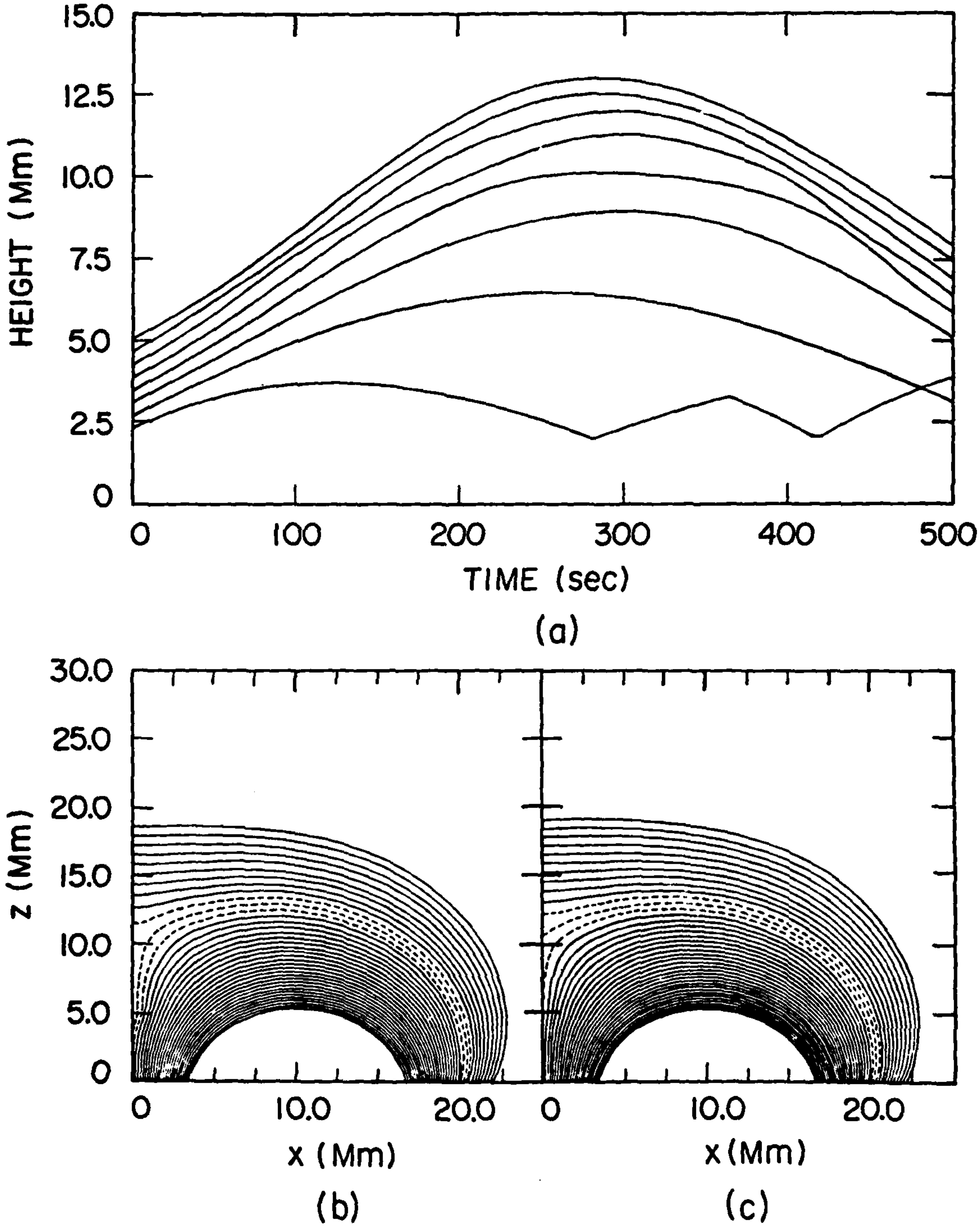
15.0
12.5
10.0
7.5
5.0
2.5
0
HEIGHT (Mm)
0
100
200
300
400
500
TIME (sec)
(a)
30.0
25.0
20.0
15.0
10.0
5.0
0
z (Mm)
0
10.0
20.0
x (Mm)
(b)
0
10.0
20.0
x (Mm)
(c)

Figure 4

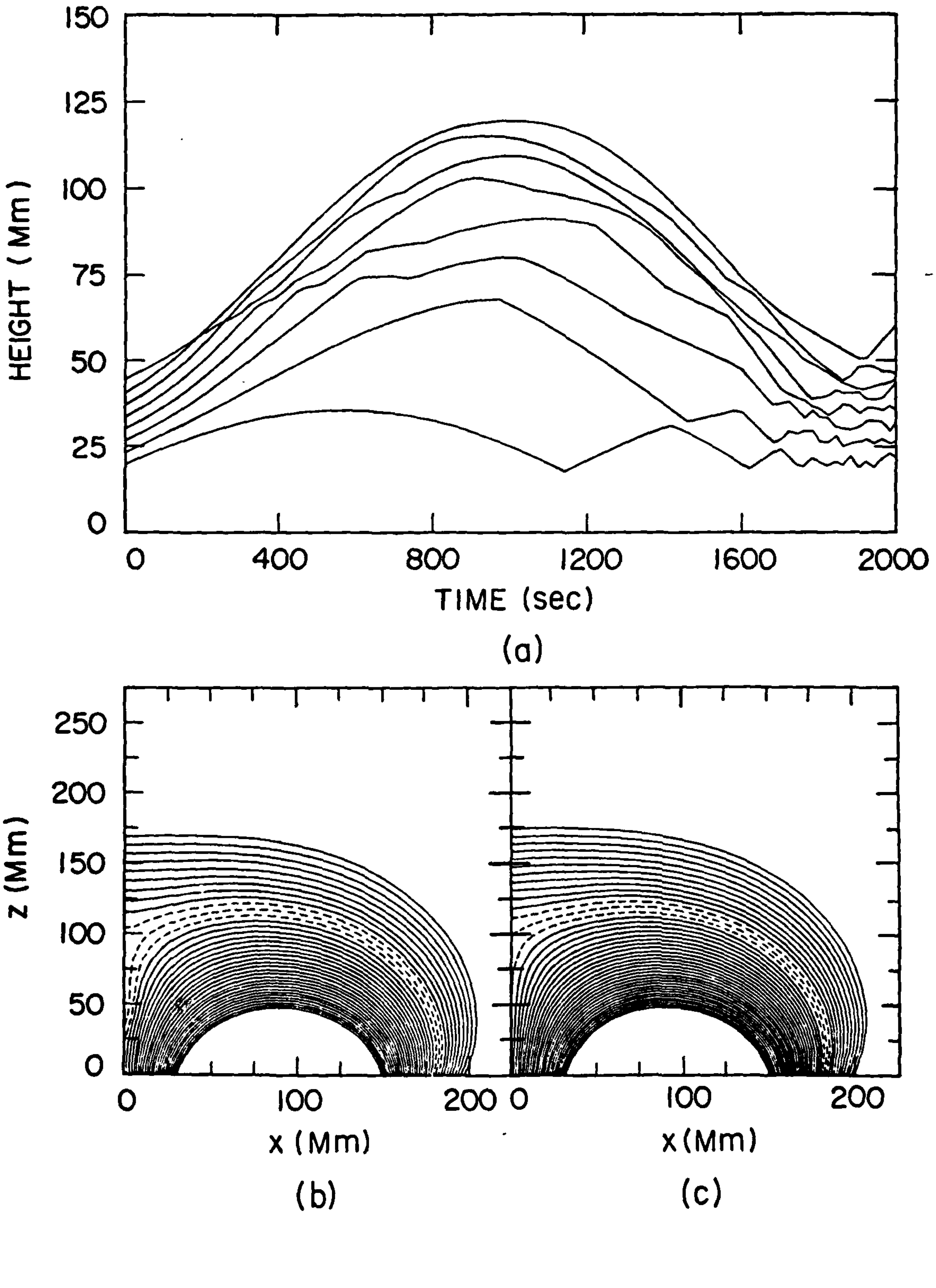
150
125
100
75
50
25
0
HEIGHT (Mm)
0
400
800
1200
1600
2000
TIME (sec)
(a)
250
200
150
100
50
0
z (Mm)
0
100
200
x (Mm)
(b)
0
100
200
x (Mm)
(c)

Figure 5

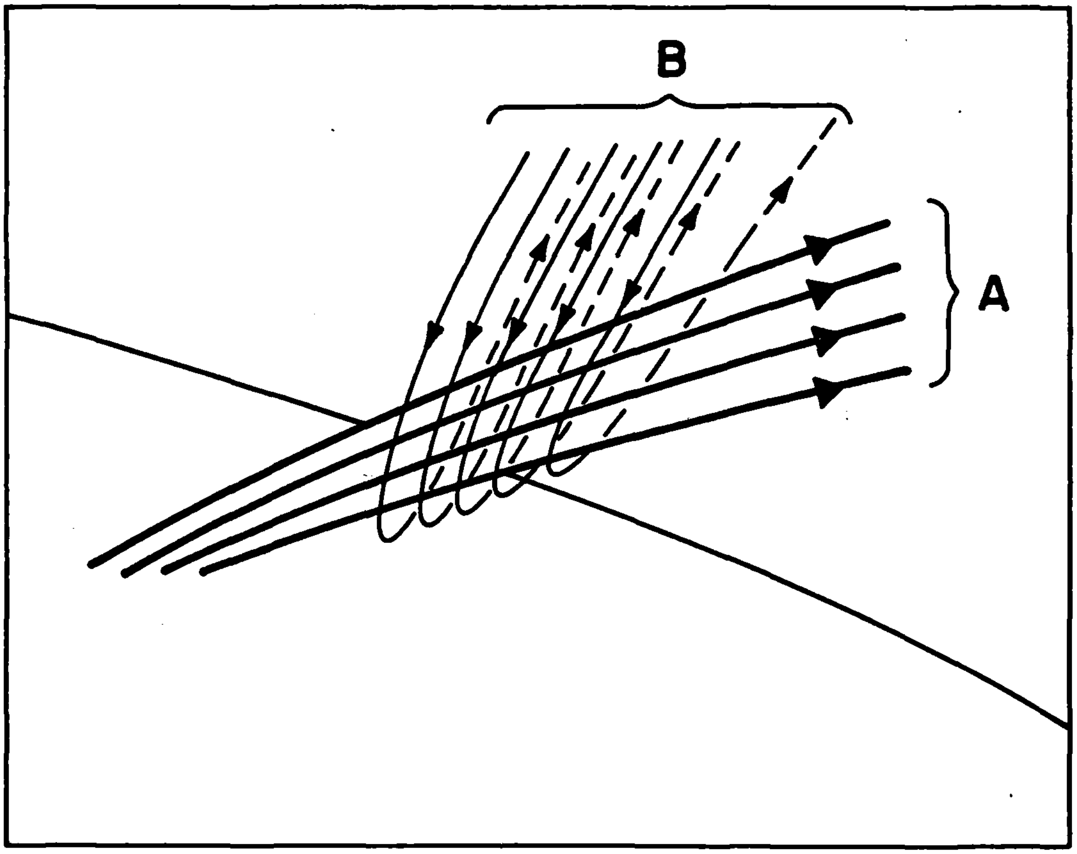

Figure 6

Plate 1

END

FILMED

[illegible] 84

DTIC